BCL6 suppresses RhoA activity to alter macrophage morphology and motility

Fiona J. Pixley[1],*, Ying Xiong[1], Raymond Yick-Loi Yu[2], Erik A. Sahai[3], E. Richard Stanley[1] and B. Hilda Ye[2],*

[1]Department of Developmental and Molecular Biology, [2]Department of Cell Biology and [3]Department of Anatomy and Structural Biology, Albert Einstein College of Medicine, 1300 Morris Park Avenue, Bronx, NY 10461, USA
*Authors for correspondence (e-mail: pixley@aecom.yu.edu; hye@aecom.yu.edu)

Summary

BCL6 is a potent transcriptional repressor that plays important roles in germinal center formation, T helper cell differentiation and lymphomagenesis and regulates expression of several chemokine genes in macrophages. In a further investigation of its role in macrophages, we show that BCL6 inactivation in primary bone marrow-derived macrophages leads to decreased polarization, motility and cell spreading accompanied by an increase in peripheral focal complexes, anchored F-actin bundles and cortical F-actin density. These changes were associated with excess RhoA activation. C3 transferase inhibition of RhoA activity reverted the adhesion structure phenotype, which was not affected by Rho kinase inhibitors, suggesting that other downstream effectors of Rho maintain this $Bcl6^{-/-}$ phenotype. Excess RhoA activation in BCL6-deficient macrophages is associated with a decrease in the p120RasGAP (RASA1)-mediated translocation of p190RhoGAP (GRLF1) to active RhoA at the plasma membrane and a reduction in cell surface expression of the CSF1R that has been reported to recruit RasGAP to the plasma membrane. Reconstitution of BCL6 expression in $Bcl6^{-/-}$ macrophages results in complete reversion of the morphological phenotype and a significant increase in cell surface CSF1R expression whereas overexpression of the CSF1R corrects the polarization and adhesion structure defects. These results demonstrate that BCL6 suppresses RhoA activity, largely through upregulation of surface CSF1R expression, to modulate cytoskeletal and adhesion structures and increase the motility of macrophages.

Key words: RhoGAP, GRLF1, RasGAP, RASA1, CSF1R, Adhesion, Spreading

Introduction

The proto-oncogene *Bcl6* encodes a transcriptional repressor that regulates the expression of a number of genes involved in leukocyte activation, proliferation and differentiation (Ye, 2000; Shaffer et al., 2002). Although high levels of BCL6 protein are found only in the lymphoid system and skeletal muscle, it is expressed at low levels in multiple cell types including macrophages (Cattoretti et al., 1995; Yamochi et al., 1997). BCL6-deficient mice demonstrate a requirement for BCL6 in the development of germinal centers and in the T-cell-dependent antibody response (Ye et al., 1997; Dent et al., 1997; Fukuda et al., 1997). These mice are growth retarded and frequently die at an early age with severe hyper-T_H2-type inflammatory disease resulting in myocarditis and acidophilic macrophage pneumonia (Ye et al., 1997; Dent et al., 1997). Although BCL6 inactivation increased the T_H2 bias of naïve CD4$^+$ T cells (Kusam et al., 2003), our previous work indicates that macrophages may also contribute to the hyper-T_H2 response seen in $Bcl6^{-/-}$ mice, possibly through increased production of several BCL6-regulated chemokines, particularly monocyte chemoattractant factor 1 (Toney et al., 2000). The finding that BCL6 regulates chemokine gene expression in macrophages also suggests that BCL6 is likely to have other gene targets and, through them, to regulate other cellular aspects of macrophage function.

In this report, we studied the regulatory role of BCL6 in macrophage adhesion and motility by examining these behaviors in BCL6-deficient bone marrow-derived macrophages (BMM). In macrophages, survival and proliferation are primarily regulated by colony stimulating factor 1 (CSF1) via the CSF1 receptor (CSF1R) (Tushinski et al., 1982; Cecchini et al., 1994; Stanley et al., 1997; Bourette et al., 2000). Together with integrins, CSF1R signaling also plays an important role in macrophage spreading, motility and focal complex formation (Boocock et al., 1989; Pixley et al., 2001; Caveggion et al., 2003). Consistent with their rapid motile response to chemotactic agents such as CSF1 (Webb et al., 1996), macrophages form small focal complexes rather than large focal adhesions upon adherence to the substratum (Pixley et al., 2001; Neumeister et al., 2003). However, macrophage focal complexes contain many of the same proteins found in focal adhesions, including paxillin, and their larger focal complexes can give rise to thin F-actin cables (Allen et al., 1997; Pixley et al., 2001). In response to CSF1 or integrin activation, paxillin is phosphorylated on tyrosine and incorporated into peripheral, nascent focal complexes or more widely distributed point contacts on the macrophage ventral surface (Neumeister et al., 2003; Suen et al., 1999).

The Rho family GTPases have been shown to regulate CSF1-induced macrophage actin reorganization, focal complex formation, motility and chemotaxis (Allen et al., 1997; Allen et al., 1998) as well as cell polarization, motility and chemotaxis in many other cell types (Ridley, 2001; Etienne-Manneville and Hall, 2002; Boettner and Van Aelst, 2002;

Meili and Firtel, 2003). Specifically, RhoA regulates the maturation of focal complexes into focal adhesions and the formation of associated stress fibers in several cell types (Rottner et al., 1999; Ridley, 2001; Burridge and Wennerberg, 2004). Several studies have shown that tail retraction, which is important for motility and possibly for polarization (Ridley et al., 2003), may be regulated by Rho (Rottner et al., 1999; Ridley, 2001; Burridge and Wennerberg, 2004) although others have demonstrated activated Rac in the retracting tail (Gardiner et al., 2002). To ensure synchronized extension/adhesion and de-adhesion/retraction cycles necessary for normal motility, activity of the Rho GTPases is coordinated by activating guanine-nucleotide exchange factors and inactivating GTPase-activating proteins (GAPs) (Ridley et al., 2003; Etienne-Manville and Hall, 2002; Moon and Zheng, 2003).

We report here that BCL6 inactivation in primary BMM leads to a decrease in cell spreading, polarization and motility accompanied by an increase in peripheral focal complexes, anchored F-actin bundles and cortical F-actin density. We further demonstrate that elevated RhoA activity is responsible for this phenotype and that reduced cell surface CSF1R expression, accompanied by decreased plasma membrane translocation of p190RhoGAP (referred to here as RhoGAP; also known as glucocorticoid receptor DNA binding factor 1, GRLF1) partly contributes to the overall phenotype.

Materials and Methods

Mice
The generation of BCL6$^{-/-}$ mice has been described previously (Ye et al., 1997). Mice used in this study were 6-12 weeks of age and maintained in a pathogen-free barrier facility. All experiments were performed according to protocols approved by the Animal Welfare Committee at the Albert Einstein College of Medicine.

Cell culture
Day 5 BMM from BCL6$^{+/+}$ and BCL6$^{-/-}$ mice were prepared as previously described (Stanley, 1990) and cultured in supplemented α-modified minimal essential medium (α+MEM) (Life Technologies) containing 15% FBS (Life Technologies, Carlsbad, CA) and 120 ng/ml human recombinant CSF1 (gift of Chiron, Emeryville, CA).

Antibodies
Antibodies used were rabbit polyclonal antibodies against Y118 phospho-paxillin (BioSource International, Camarillo, CA) and p27 RhoGAP (a gift from Sally Parsons, University of Virginia), mouse monoclonal antibodies against RhoA, RasGAP (Santa Cruz Biotechnology, Santa Cruz, CA), a goat polyclonal anti-CSF1R antibody (Wang et al., 1999) and a rat monoclonal anti-CSF1R antibody (a gift from S. Shinikawa) (Sudo et al., 1995). Rhodamine-conjugated phalloidin (Molecular Probes, Eugene, OR) was used for F-actin staining.

Microscopy
For light microscopy, BMM were plated on fibronectin-coated glass coverslips (BD Biosciences, Palo Alto, CA), grown to 60-70% confluence in the presence of CSF1. For CSF1 stimulation experiments, cells were starved of CSF1 for 24 hours prior to addition of CSF1 (120 ng/ml). The cells were then rinsed with PBS and fixed in 3.7% formaldehyde for 5-10 minutes then examined by phase contrast using an Olympus inverted microscope or permeabilized with

0.5% Triton X-100 and prepared for immunofluorescent staining as previously described (Pixley et al., 2001). For spreading assays after replating, cells were seeded for the indicated times and then gently rinsed twice with PBS before fixation and staining. The coverslips were mounted in ProLong Antifade reagent (Molecular Probes), and all samples were examined under an Olympus 1X70 inverted microscope with images recorded using a Photometrics CH1 CCD camera and/or a BioRad Radiance 2000 laser-scanning confocal microscope. Interference reflection microscopy (IRM) was performed using a 60× 1.4 NA planapo Nikon infinity-corrected objective with the BioRad confocal microscope and the results analyzed as previously described (Neumeister et al., 2003). Quantification of cell polarization (Fig. 1E), pseudopodial numbers/cell (Fig. 1F) and cell footprint area (Fig. 4C) were carried out on either F-actin-stained or IRM samples, with polarization determined from the maximum length/maximum width ratio given by the 'best fit' ellipse for each cell, using ImageJ software (NIH, Bethesda, MA). As $n>30$ in each case, statistical analyses were based on the normal distribution. For scanning EM, cells were fixed in 1% osmium tetroxide/0.1 M cacodylate for 5 seconds at 22°C followed by 2.5% glutaraldehyde/0.1 M cacodylate as previously described (Pixley et al., 2001). Dehydrated cells were critical-point dried using liquid carbon dioxide in a Tousimis Samdri 790 critical-point drier, sputter-coated with gold-palladium in a Denton Vacuum Desk-1 sputter-coater, mounted, and viewed in a JEOL JSM6400 scanning electron microscope using an accelerated voltage of 10 kV for EM. BMM for cytoskeletal preparations were grown to 60% confluence on 6 mm glass coverslips and subjected to CSF1 stimulation as described above. Platinum replicas of BMM cytoskeletons were prepared as previously described (Svitkina et al., 1995) with the following modifications. Briefly, after rinsing with PBS at 37°C, BMM were extracted for 2 minutes at 37°C in PHEM buffer (60 mM PIPES, 25 mM HEPES, 10 mM EGTA, 2 mM MgCl$_2$, pH 6.9) with 2 μM phallacidin (Molecular Probes), 10 μg/μl leupeptin and aprotinin, 1 mM benzamidine and 0.75% Triton X-100 then rinsed in PHEM buffer with 0.1 μM phallacidin for 1 minute before a 10-minute fixation in 1% glutaraldehyde/0.1 μM phallacidin/PHEM buffer. After a final rinse in HPLC grade water with 0.1 μM phallacidin, the coverslips were rinsed three times in water and processed as previously described (Hartwig, 1992). The samples were observed using a JEOL 100CX transmission EM at 100 kV. By convention, images were viewed as negatives.

Motility assays
For Boyden Chamber motility assays, 1×10^5 cells were seeded into 8 μm pore size inserts (BD Biosciences) in the presence (chemokinesis) or absence (chemotaxis) of CSF1 and the inserts placed in CSF1-supplemented lower wells. Migration was measured after 3 hours by counting cells on the underside of the insert membrane after 3.7% formaldehyde fixation and haematoxylin staining. The number of migrated cells was normalized to the number of cells directly plated in an insert-free well and assays were performed in triplicate.

Rho activation and Rho and Rho-associated protein kinase 1 (ROCK1) inhibition assays
An activated RhoA pull-down kit was purchased from Cytoskeleton and assays performed as directed by supplied protocols. Briefly, subconfluent BMM cultures were starved of CSF1 for 24 hours then re-stimulated for either 0 or 20 minutes before an ice-cold PBS rinse and lysis in 500 μl of the supplied lysis buffer supplemented with 0.5% sodium deoxycholate and 0.1% SDS for improved cell lysis. Equal volumes of supernatants were incubated with Rhotekin-RBD affinity beads (Ren et al., 1999) for 1 hour at 4°C, followed by two washes in lysis buffer and three washes in the supplied wash buffer. Bound proteins were eluted in 3× 1% SDS sample buffer and

examined by 15% SDS-PAGE and western blot analysis. For Rho and ROCK1 inhibition, subconfluent cells plated on fibronectin-coated coverslips were either exposed to a cell penetrant, Tat-tagged form of C3 toxin at 0.5 μM overnight as previously described (Coleman et al., 2001) or treated for 30 minutes prior to fixation with either 10 μM Y27632 or 5 μM HA 1077 (Calbiochem, San Diego, CA). The cells were then fixed, permeabilized and stained for Y118 phospho-paxillin as described above.

Retroviral infection

The coding region of either human BCL6 cDNA or mouse CSF1R cDNA was inserted into the MSCV-IRES-GFP vector (Persons et al., 1999) at the *Eco*RI site upstream of the IRES driving expression of GFP. MSCV retroviruses were prepared by transient co-transfection with the ecotropic, replication-defective helper virus, pSV-Ψ–E-MLV (Muller et al., 1991), as described previously (Neumeister et al., 2003). The retroviruses were gifts of A. W. Nienhuis (St Jude Children's Research Hospital, Memphis, TN) and O. N. Witte (UCLA, Los Angeles, CA), respectively. Wild-type and *Bcl6*^{-/-} BMM were incubated with fresh retroviral supernatants in the presence of 120 ng/ml of CSF1 and 4 μg/ml of polybrene for 24 hours and cultured for 36 hours before fluorescence-activated cell sorting (FACSVantage SE, Becton Dickinson) for GFP^{+} cells. Sorted GFP^{+} cells were used for morphological and immunofluorescent analyses.

Immunoprecipitation and western blotting

Subconfluent BMM cultures were rinsed in ice-cold PBS and scraped in either 200 μl lysis buffer (10 mM Trizma Base, 50 mM NaCl, 30 mM sodium pyrophosphate, 50 mM NaF, pH 7.0 containing 5 μM $ZnCl_2$, 0.5 mM sodium orthovanadate, 0.5% NP-40, 1 mM benzamidine, 10 μg/ml leupeptin, 10 μg/ml aprotinin) at 4°C and prepared for immunoprecipitation as previously described (Pixley et al., 2001) or scraped in 200 μl 1% SDS sample buffer for whole cell lysates. Protein concentrations were determined by BCA protein assay (Pierce, Rockford, IL) and protein samples were analyzed by 8% SDS-PAGE and western blotting as previously described (Pixley et al., 2001). Equal lysate protein loading was confirmed by detecting GAPDH.

Flow cytometric analysis

Approximately 2×10^5 BMM were incubated at 4°C for 30 minutes with 1 μg/ml of either biotinylated anti-CSF1R antibody (directed to the extracellular domain of the CSF1R) or isotype-matched control IgG (BD Pharmingen). Labeled cells were washed twice with PBS containing 1% BSA and incubated with phycoerythrin-conjugated streptavidin (BD Pharmingen) at 4°C for 30 minutes, washed as above, and analyzed on a fluorescent-activated cell scanner (FACScan, Becton Dickinson).

Results

Bcl6^{-/-} macrophages display altered cell morphology

When cultured in the presence of CSF1, *Bcl6*^{-/-} BMM were less likely to be bipolar than their wild-type (WT) counterparts, frequently displaying either a multipolar stellate morphology or, less often, an apolar circular phenotype (Fig. 1A-D). In addition, scanning EM revealed that the majority of *Bcl6*^{-/-} BMM possessed large numbers of small apical membrane protrusions (Fig. 1D) that did not resemble the dorsal ruffles seen in WT BMM (Fig. 1C). Quantitative analysis of mean cell polarization demonstrated a significant reduction in the polarity index of *Bcl6*^{-/-} BMM (1.80±0.16 compared to

3.29±0.24 for *Bcl6*^{+/+} BMM, Fig. 1E). To quantify the two phenotypes noted in *Bcl6*^{-/-} BMM more accurately (Fig. 1B,D), the number of pseudopodia per cell were scored. Although the majority (68%) of *Bcl6*^{+/+} BMM were bipolar and only 27% extended three or more pseudopodia, 65% of *Bcl6*^{-/-} BMM displayed three or more pseudopodia and the remaining cells were more likely to be circular (polarization index <1.5; 18%) than their WT controls (5%) (Fig. 1F). Under time-lapse video microscopy, some cycling *Bcl6*^{-/-} BMM were seen to change from one phenotype to the other during the 90 minute observation period (data not shown).

Bcl6^{-/-} macrophages display altered adhesion and F-actin structures

To investigate the basis of the morphological alterations in *Bcl6*^{-/-} BMM, we examined the F-actin cytoskeleton and focal complexes in the WT and *Bcl6*^{-/-} BMM by immunofluorescence microscopy. Staining for the focal complex marker, Y118 phospho-paxillin (Pixley and Stanley,
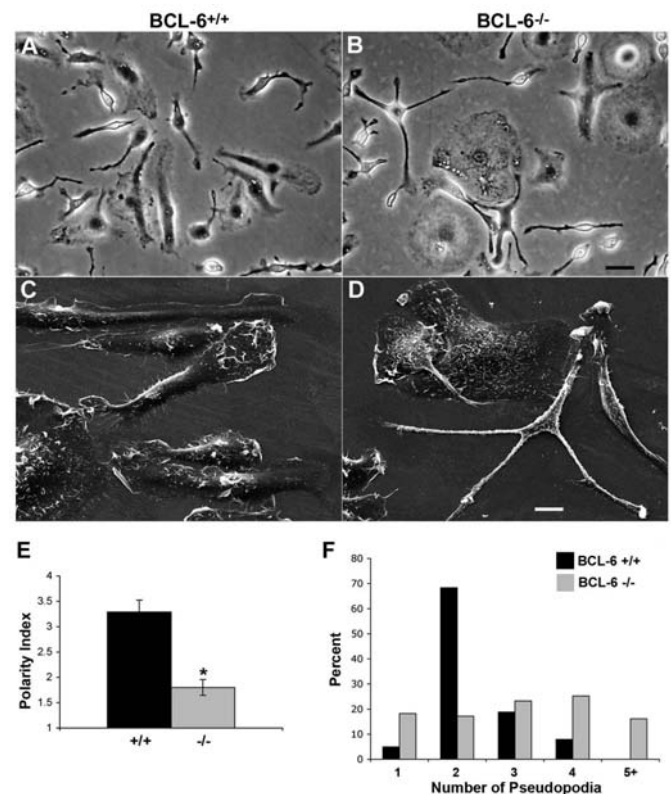

Fig. 1. *Bcl6*^{-/-} macrophages have a morphology distinct from that of *Bcl6*^{+/+} BMM. BMM were plated on tissue culture plastic (A,B) and fibronectin-coated coverslips (C,D) and grown to subconfluence in the presence of CSF1 before fixation. Phase-contrast (A,B) and scanning EM (C,D) images of *Bcl6*^{+/+} (A,C) and *Bcl6*^{-/-} BMM (B,D). (E) Polarization indices of *Bcl6*^{+/+} (+/+) and *Bcl6*^{-/-} (–/–) BMM (Polarization index=ratio of maximum cell length to maximum cell width, n>30; error bars represent s.e.m.; *P<0.001 significantly different from the index in *Bcl6*^{+/+} BMM cells). (F) Numbers of pseudopodia per cell in *Bcl6*^{+/+} and *Bcl6*^{-/-} BMM (for maximum cell length/maximum cell width ratio ≤1.5, pseudopodia count=1; n=100). Bar, 20 μm (A,B); 10 μm (C,D).

2004), revealed that *Bcl6*^{−/−} BMM displayed more peripherally positioned and frequently circumferential focal complexes than WT BMM (Fig. 2D, open arrowhead). In contrast, WT BMM displayed many small phospho-paxillin-rich point contacts
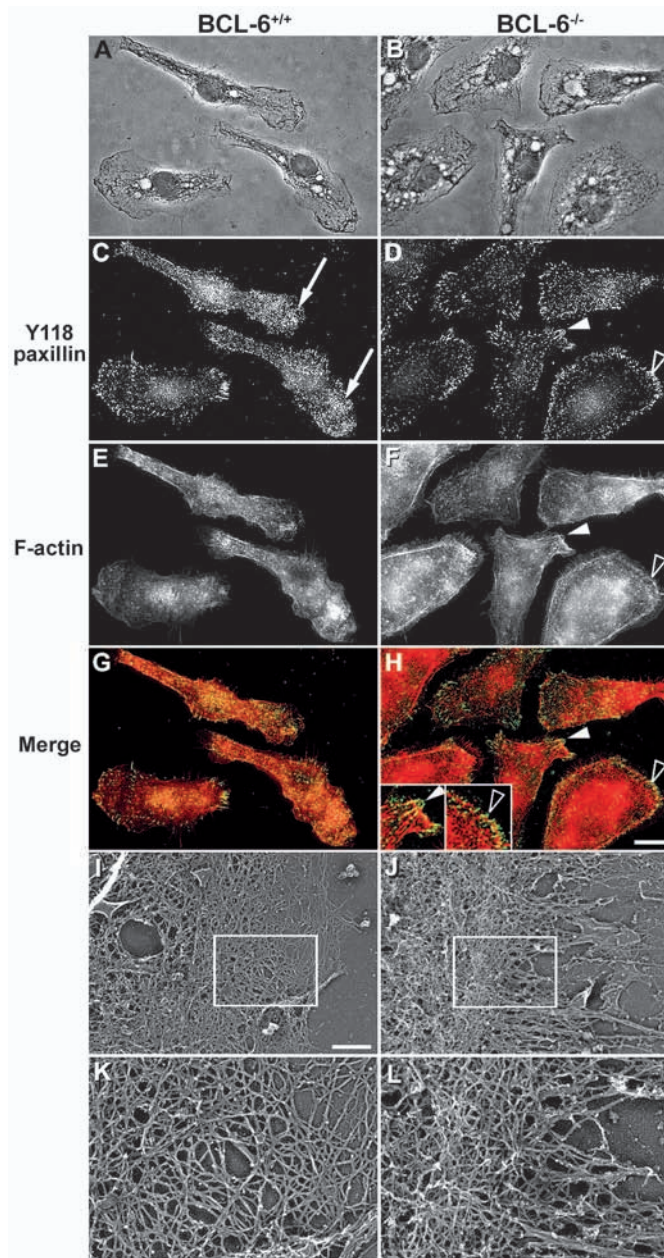

Fig. 2. *Bcl6*^{−/−} macrophages display altered focal complex and F-actin structures. *Bcl6*^{+/+} (A,C,E,G,I,K) and *Bcl6*^{−/−} BMM (B,D,F,H,J,L) were plated on fibronectin-coated coverslips, grown to subconfluence in the presence of CSF1, then starved of CSF1 for 24 hours prior to re-stimulation for 20 minutes. Immunofluorescence samples (A-H) were stained for Y118 paxillin (C,D; green in merged fields G,H) and F-actin (E,F; red in merged fields). Arrows indicate dense collections of phospho-paxillin-rich point contacts, closed arrowheads indicate focal complexes that subtend F-actin bundles, and open arrowheads indicate circumferential focal complexes with overlying F-actin belts. Inserts in H highlight the focal complexes and F-actin structures. (I,J) Representative cytoskeletal replicas. (K,L) Enlarged regions framed in I and J. Bar, 10 μm (A-H); 500 nm (I,J).

(Tawil et al., 1993) over the ventral surface and often more concentrated under leading lamellipodia (Fig. 2C, arrows). These point contacts were only infrequently observed in *Bcl6*^{−/−} BMM (Fig. 2D). Instead, *Bcl6*^{−/−} BMM often displayed dense, circumferential F-actin staining (Fig. 2F) that colocalized with the circumferential focal complexes (Fig. 2H, open arrowhead) as well as thick F-actin cables that could clearly be seen to arise from large focal complexes (Fig. 2D,F,H, closed arrowheads). Thick actin bundles with associated anchoring focal complexes were rarely seen in WT BMM (Fig. 2C,E,G). These differences were evident in BMM either stimulated with CSF1 for 20 minutes (Fig. 2) or grown in the continuous presence of CSF1 (data not shown) although the larger focal complexes and F-actin cables were more evident in CSF1-stimulated cells. To reveal detailed cortical actin structures, platinum-coated cytoskeletal replicas of WT and *Bcl6*^{−/−} BMM were examined under transmission EM. The cortical actin ring noted in many *Bcl6*^{−/−} BMM was shown to be due to an increased density of the lamellipodial orthogonal F-actin network rather than bundling of circumferentially arranged actin filaments (Fig. 2I-L).

Motility is reduced in *Bcl6*^{−/−} macrophages

The peripheral focal complexes, associated actin bundles and condensed lamellipodial networks strongly suggested that *Bcl6*^{−/−} BMM might be less motile than WT BMM, and initial experiments indicated that they moved more slowly to close a wounded confluent monolayer than the WT controls (data not shown). In a more quantitative, Boyden chamber-based motility assay, *Bcl6*^{−/−} BMM displayed reduced migration whether assessed for random motility (chemokinesis, 33.7% of WT) or chemotaxis to CSF1 (57.8% of WT) (Fig. 3).

Loss of BCL6 leads to delayed macrophage spreading and altered focal complex remodeling

As observation of macrophage spreading after replating may reveal spreading defects that are less readily seen following CSF1 stimulation, replated WT and *Bcl6*^{−/−} BMM were examined at various times from 15 minutes to 24 hours after replating. In addition to the morphology and motility defects described above, *Bcl6*^{−/−} BMM also exhibited delayed spreading after replating on fibronectin (Fig. 4), collagen and laminin (data not shown). The footprint areas of WT and *Bcl6*^{−/−} BMM spreading on fibronectin were determined from IRM images of cells fixed at intervals from 15 minutes to 24 hours after replating. Spreading of the *Bcl6*^{−/−} BMM was significantly delayed, with a 50% reduction in their footprint area still evident 8 hours after replating, compared to WT BMM, although both cell types were equally spread by 24 hours (Fig. 4A,C). Moreover, although both cell types initially spread in a circular manner, WT BMM began to polarize by 2 hours whereas *Bcl6*^{−/−} BMM showed no sign of polarization by 4 hours and either remained circular or developed multiple pseudopodia with few lamellipodia (Fig. 4A). To investigate whether *Bcl6*^{−/−} BMM were forming appropriate adhesion structures during spreading, we examined the distribution of ventral surface phospho-paxillin in WT and mutant BMM after replating. WT BMM displayed widely distributed phospho-paxillin-rich point contacts over the entire ventral surface (Fig.
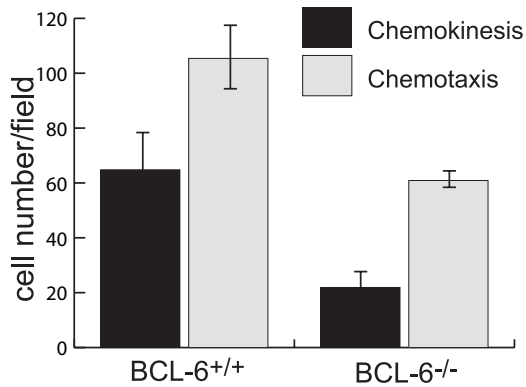
Fig. 3. *Bcl6⁻/⁻* macrophages have reduced motility. Approximately 1×10^5 BMM were added to 8 μm pore-size inserts in either the presence (chemokinesis, black bars) or absence (chemotaxis, gray bars) of CSF1 and then placed in CSF1-containing wells for 3 hours. Migrated cells were scored and normalized to the total cell number in an insert-free well. The means of four fields per insert were averaged and the results shown are representative of three independent experiments (mean±s.e.m.). Differences in proliferation rates (unpublished data) would not have significantly contributed to the results of this 3-hour experiment.

4B) whereas spreading *Bcl6⁻/⁻* BMM developed distinct and frequently large focal complexes at their peripheral margins (Fig. 4B) and, at later time points, at their pseudopodial tips (data not shown). As organized focal complexes form inap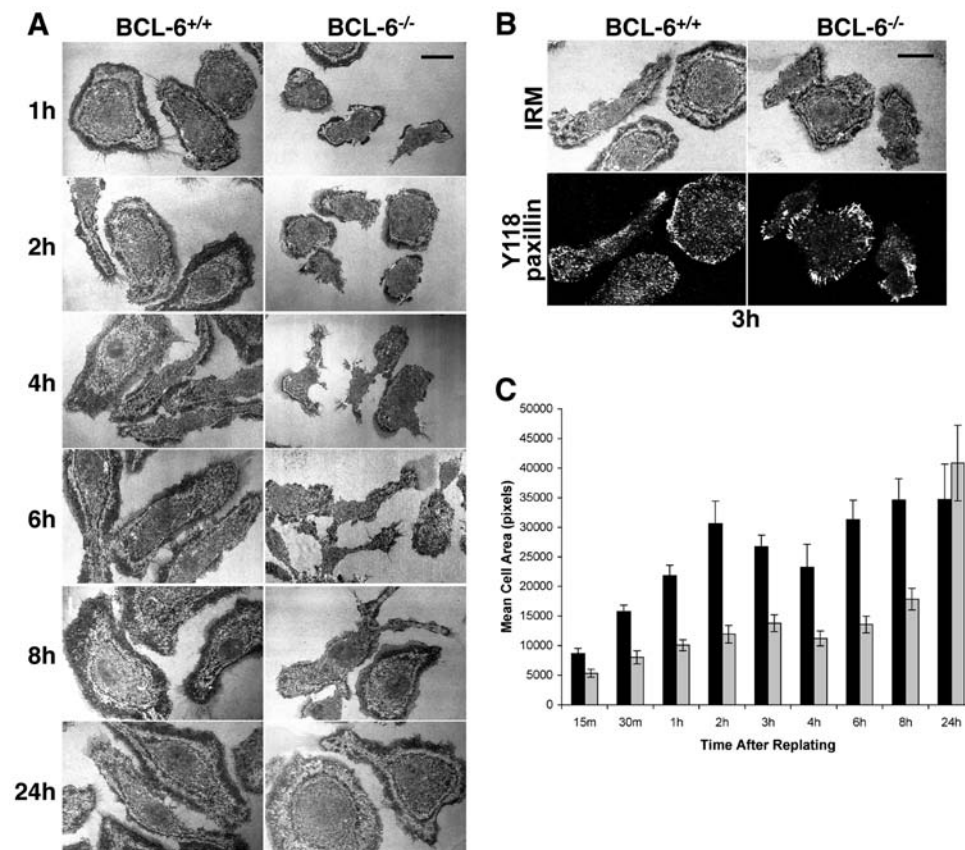propriately early in spreading *Bcl6⁻/⁻* BMM and these cells lack the widely spread point contacts commonly found in WT BMM, remodeling of adhesion structures appears to be dysregulated in the absence of BCL6, leading to delayed spreading.

RhoA activation is increased in *Bcl6⁻/⁻* macrophages

RhoA activation converts focal complexes into larger focal adhesions and increases the numbers of stress fibers arising from these focal adhesions in many cell types (Ridley, 2001; Etienne-Manneville and Hall, 2002; Moon and Zheng, 2003). Although macrophages do not form focal adhesions or actin stress fibers, the increased formation of focal complexes and organized F-actin structures in *Bcl6⁻/⁻* BMM suggested an increase in RhoA activity. Moreover, RhoA has been shown to regulate the formation of apical membrane protrusions in fibroblasts (Shaw et al., 1998) reminiscent of those seen in *Bcl6⁻/⁻* BMM (Fig. 1D, cells in upper left corner). To determine whether the large focal complexes with anchored actin bundles and circumferential cortical actin 'belts' in *Bcl6⁻/⁻* BMM were due to alterations in Rho activation, we measured Rho activity in WT and *Bcl6⁻/⁻* BMM using Rhotekin-RBD affinity beads. Activated RhoA was recovered from unstimulated and 20 minutes CSF1-stimulated WT and *Bcl6⁻/⁻* BMM lysates. At both time points significantly greater amounts of activated RhoA were recovered from *Bcl6⁻/⁻* BMM compared to WT cells (Fig. 5). In addition, although Rho activity increased in WT BMM following CSF1 stimulation, this increase was not evident in the *Bcl6⁻/⁻* BMM (Fig. 5). In contrast, no difference in Rac or Cdc42 activation was observed between WT and *Bcl6⁻/⁻* BMM (data not shown). These results indicate that RhoA, irrespective of CSF1 stimulation, is specifically activated in *Bcl6⁻/⁻* BMM at higher levels than in WT macrophages. As loss of polarization occurs in *Bcl6⁻/⁻* BMM and Rho has been reported to be highly concentrated in the trailing uropod in neutrophils (Xu et al., 2003), we carried out IF staining for RhoA in WT and
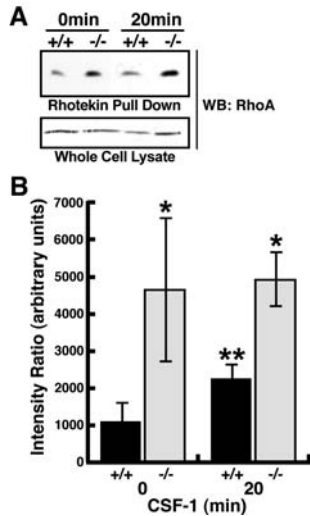

Fig. 4. Spreading is delayed in *Bcl6⁺/⁺* macrophages and is associated with altered focal complex remodeling. *Bcl6⁺/⁺* and *Bcl6⁻/⁻* BMM were plated on fibronectin-coated coverslips for the indicated times, fixed and examined by confocal microscopy. (A) BMM fixed 1, 2, 4, 6, 8 and 24 hours after plating and examined by interference reflection microscopy. (B) BMM fixed 3 hours after plating and examined by IRM and immunofluorescence staining for phosphoY118 paxillin. (C) Analysis of mean cell footprint areas at 15 and 30 minutes, 1, 2, 4, 6, 8 and 24 hours (*Bcl6⁺/⁺*, black, *Bcl6⁻/⁻*, gray; mean±s.e.m. of cells in six fields). Bar, 10 μm.

Fig. 5. RhoA is hyper-activated in *Bcl6*⁻/⁻ macrophages. (A) A GST-Rhotekin-RBD pull-down assay was performed on WT and *Bcl6*⁻/⁻ BMM stimulated with CSF1 for 0 and 20 minutes. Eluted proteins were examined by western blotting for associated active RhoA. Bottom panel demonstrates equivalent presentation of input protein as determined by RhoA western blotting of 30 µg RIPA lysates from the above samples. (B) Bar graph summarizes the results from three independent GST-Rhotekin-RBD pull-down assays (mean±s.d.; *$P<0.05$ significantly different from intensity in *Bcl6*⁺/⁺ BMM at 0 or 20 minutes; **$P<0.05$, significantly different from intensity in *Bcl6*⁺/⁺ BMM at 0 minute).

Bcl6⁻/⁻ BMM. However, we failed to detect any polarization in the subcellular distribution of total RhoA protein in either WT or *Bcl6*⁻/⁻ BMM (data not shown).

Reversion of morphological abnormalities in *Bcl6*⁻/⁻ macrophages by BCL6 reconstitution or inhibition of Rho but not Rho-kinase

To determine whether the morphological alterations in *Bcl6*⁻/⁻ BMM were reversible regulatory defects or consequences of irreversible abnormalities in macrophage differentiation, BCL6 was re-expressed in *Bcl6*⁻/⁻ BMM by retroviral transduction. Infected, GFP-expressing *Bcl6*⁻/⁻.*Bcl6* BMM were sorted by FACS and the actin cytoskeleton and ventral surface adhesion structures examined by IF analysis. There was a close correlation between BCL6 expression (correlated with GFP expression), repolarization and return of ventral surface point contacts with a concurrent disappearance of the peripheral, large focal complexes (Fig. 6A-C). Quantification of cell polarization confirmed the re-polarization of *Bcl6*⁻/⁻ BMM upon restoration of BCL6 expression (Fig. 6D). These results indicate that the morphological abnormalities in *Bcl6*⁻/⁻ BMM are caused by reversible regulatory defects rather than the result of a permanently altered differentiation state. Moreover, appropriate interference could identify which molecules act downstream of BCL6 to maintain this phenotype.

As transcription factors have multiple targets, excess RhoA activation may or may not play a major role in the described changes. To delineate the contribution of RhoA, *Bcl6*⁺/⁺ and *Bcl6*⁻/⁻ BMM were treated with either a cell penetrant form of
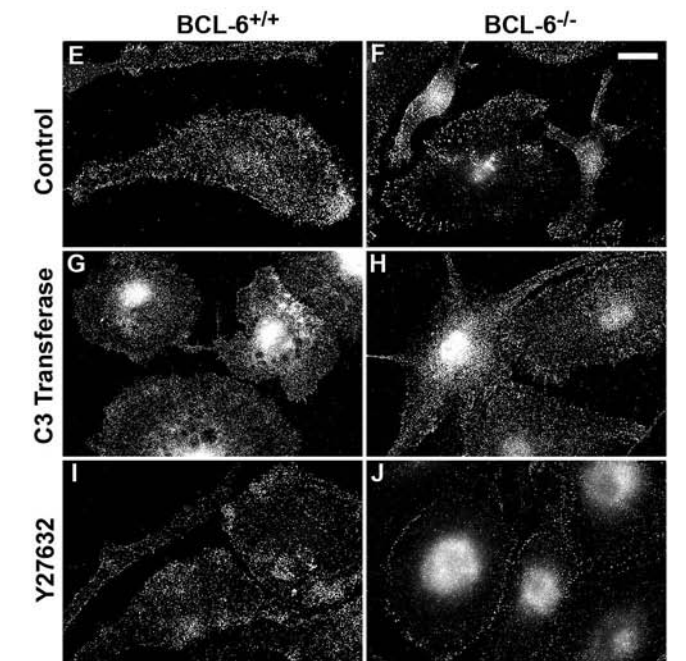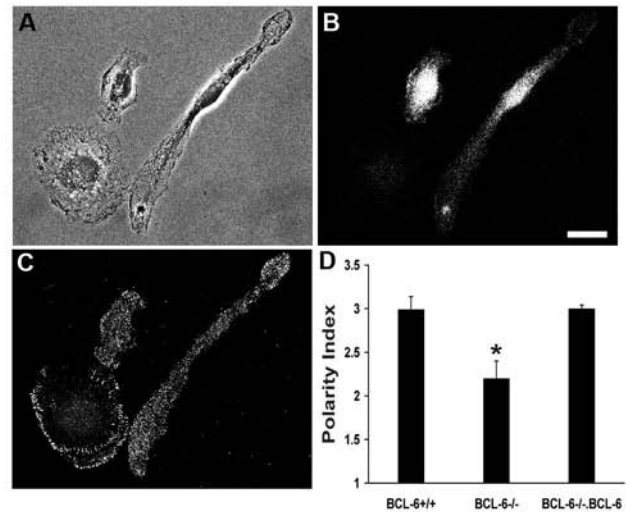

Fig. 6. Reconstitution of BCL6 expression and RhoA inhibition each cause phenotypic reversion of ventral surface adhesion structures and repolarization. (A-D) A BCL6 expression construct was retrovirally transduced into *Bcl6*⁻/⁻ BMM and the cells sorted for GFP expression 36 hours post-infection. GFP-positive cells were plated on fibronectin-coated coverslips for 24 hours before fixation and staining for Y118 paxillin (C) and visualization of GFP expression (B). (D) Quantification of polarization indices for *Bcl6*⁺/⁺, *Bcl6*⁻/⁻ BMM and BCL6-reconstituted *Bcl6*⁻/⁻ BMM (error bars, s.e.m.; *$P<0.02$ significantly different from index in *Bcl6*⁺/⁺ BMM cells). (E-J) *Bcl6*⁺/⁺ and *Bcl6*⁻/⁻ BMM were treated with either TBS buffer (control, E,F), Tat-tagged C3 transferase (G,H) or the ROCK1 inhibitor, Y27632 (I,J) before fixation and staining for Y118 paxillin. Treatment with another ROCK1 inhibitor, HA 1077, produced similar results to Y27632 treatment (not shown). Bar, 10 µm.

C3 transferase to inhibit Rho activity or inhibitors (Y27632, HA 1077) of ROCK1, a known Rho effector, prior to fixation and staining for Y118 phospho-paxillin. Lysates from C3 transferase-treated cells were examined by Rho Western

blotting and showed retarded electrophoretic mobility, consistent with ADP ribosylation of Rho protein (data not shown). Direct inhibition of RhoA resulted in increased spreading with either a loss of polarization or failure of tail retraction in both WT and *Bcl6⁻/⁻* BMM, as has been shown in monocytes treated with C3 transferase (Allen et al., 1997; Worthylake et al., 2001) (Fig. 6G,H). In the C3 transferase-treated *Bcl6⁻/⁻* BMM, however, there was a clear increase in the number of phospho-paxillin-rich point contacts and a loss of peripheral focal complexes such that their ventral surface phospho-paxillin distribution resembled that seen in normal and C3 transferase-treated WT BMM (Fig. 6H). In contrast, ROCK1-inhibited *Bcl6⁻/⁻* BMM continued to display peripheral focal complexes with few ventral surface point contacts (Fig. 6I,J), although ROCK1 inhibition did lead to elongated tail formation, as was seen following C3 transferase treatment, and translocation of Y118 phospho-paxillin to the perinuclear region. Thus, elevated RhoA activity in *Bcl6⁻/⁻* BMM was responsible for the dysregulation of adhesion complex formation and these Rho-mediated adhesion effects were ROCK1-independent. As C3 transferase inhibition of RhoA caused complete loss of cell polarity, even in WT BMM, the origin of the polarization defects in *Bcl6⁻/⁻* BMM could not be determined in this assay.

RhoGAP and RasGAP association and translocation to the plasma membrane are reduced in *Bcl6⁻/⁻* macrophages

Active RhoA is associated with the plasma membrane (Bokoch et al., 1994) and is inactivated by RhoGAP (Ellis et al., 1990), causing loss of stress fibers and focal adhesions (Moon and Zheng, 2003). RhoGAP associates with p120RasGAP (referred to here as RasGAP; also known as Ras GTPase-activating protein 1, RASA1) and translocation of the active RasGAP/RhoGAP complex to the plasma membrane has been shown to be important in the regulation of RhoA by RhoGAP (McGlade et al., 1993; Trouliaris et al., 1995; Dib et al., 2001). Thus, we examined the subcellular distribution of RhoGAP and RasGAP in WT and *Bcl6⁻/⁻* BMM by IF staining, using F-actin staining to delineate the ruffles (Fig. 7). In WT BMM, RhoGAP was clearly localized to the dorsal ruffles (Fig. 7A,C), whereas there was only faint RhoGAP staining in the dorsal ruffles of *Bcl6⁻/⁻* BMM (Fig. 7B,D). Consistent with the altered RhoGAP localization in *Bcl6⁻/⁻* BMM, RasGAP staining in dorsal ruffles of these cells was also reduced compared with WT BMM (Fig. 7E,F), suggesting reduced plasma membrane localization of both proteins in *Bcl6⁻/⁻* BMM and, therefore, reduced access of RhoGAP to active, plasma membrane-associated RhoA. Western blotting followed by densitometric analysis of RhoGAP and RasGAP signals after subcellular fractionation of *Bcl6⁺/⁺* and *Bcl6⁻/⁻* BMM indicated a 31% reduction in the amount of membrane-associated RhoGAP in *Bcl6⁻/⁻* BMM compared with WT BMM and a 40% reduction in membrane-associated RasGAP from *Bcl6⁻/⁻* BMM compared with WT BMM although the levels of total RhoGAP and RasGAP are unaltered in *Bcl6⁻/⁻* BMM (data not shown). In addition, RasGAP immunoprecipitations showed a reduced association of RhoGAP with RasGAP in *Bcl6⁻/⁻* BMM (data not shown). Thus, the amount of RhoGAP present at the plasma membrane is reduced in *Bcl6⁻/⁻* BMM and this
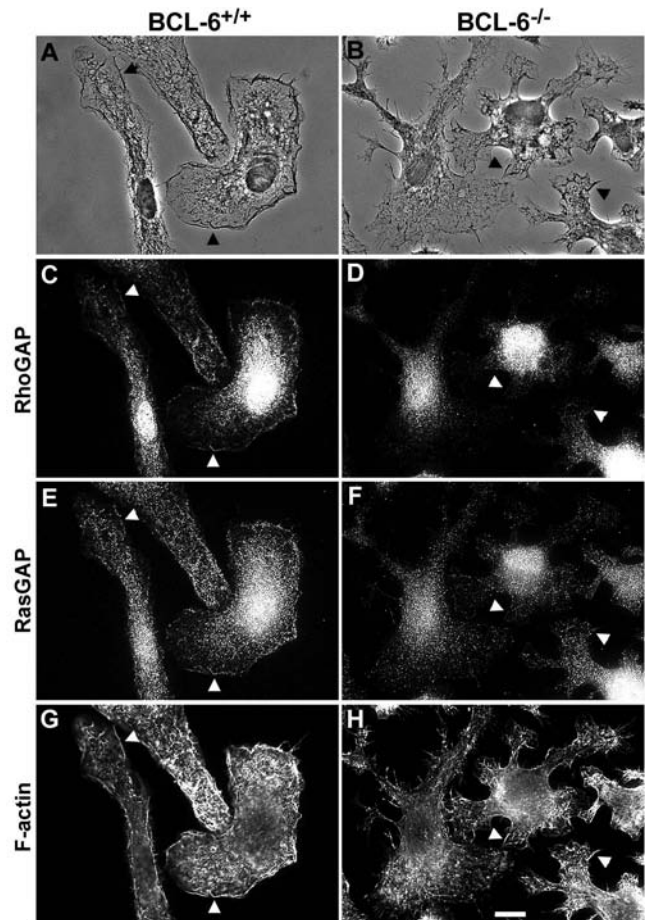

Fig. 7. RhoGAP and RasGAP levels are reduced at the plasma membrane in *Bcl6⁻/⁻* macrophages. RhoGAP (C and D) and RasGAP (E and F) colocalize at the plasma membrane and membrane localization of each was reduced in *Bcl6⁻/⁻* BMM. Arrowheads highlight plasma membrane ruffles, visualized by phase contrast (A and B) and F-actin staining (G and H). Bar, 10 µm.

reduction is likely to result from reduced association of RhoGAP with RasGAP and decreased translocation of the RasGAP/RhoGAP complex.

The CSF1R colocalizes with RasGAP and RhoGAP at the plasma membrane and exhibits reduced surface expression in *Bcl6⁻/⁻* macrophages

It has been reported that RasGAP may be recruited to the plasma membrane through association with activated CSF1R protein complexes (Trouliaris et al., 1995; Berg et al., 1999) and that this recruitment regulates cell morphology (Trouliaris et al., 1995). Thus, we investigated the association of both RasGAP and RhoGAP with the CSF1R in WT BMM and found plasma membrane colocalization of these proteins was reduced in *Bcl6⁻/⁻* BMM (RhoGAP, Fig. 8A-F; RasGAP, data not shown). Moreover, diminished CSF1R staining at the plasma membrane of *Bcl6⁻/⁻* BMM suggested reduced surface expression of the receptor (Fig. 8E,F). Indeed, Western blotting indicated that there was a marked reduction in expression of the mature 165 kDa form of the CSF1R compared to the immature 130 kDa form in *Bcl6⁻/⁻* BMM (Fig. 8G). Consistent
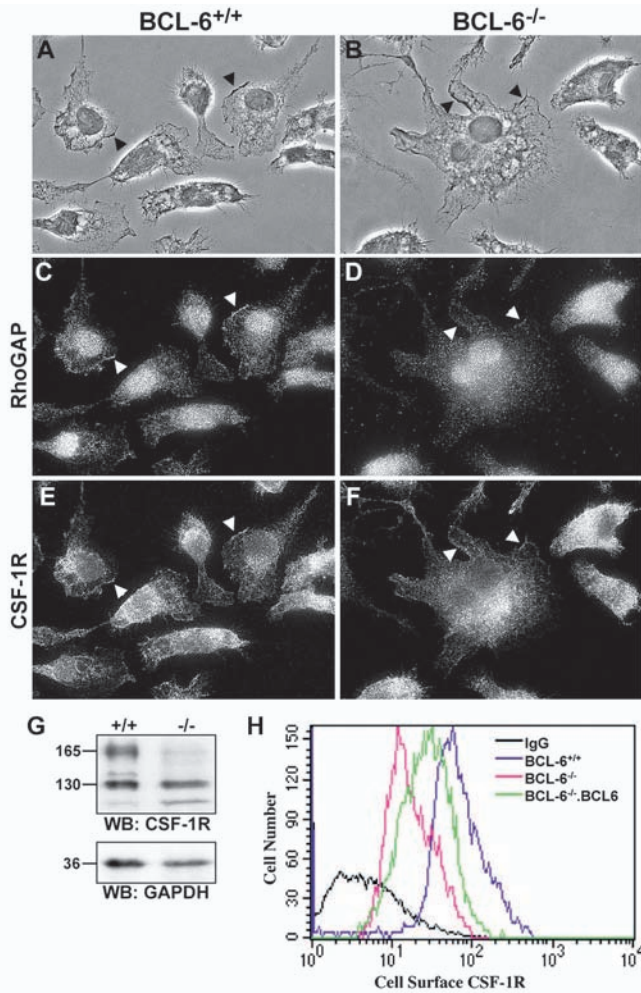
Fig. 8. Surface CSF1R expression and colocalization with RhoGAP is reduced in *Bcl6*−/− macrophages. RhoGAP (C and D) colocalizes with the CSF1R (E and F) at the plasma membrane. Localization of RhoGAP and the CSF1R to the plasma membrane both appear reduced in *Bcl6*−/− BMM. Up to 20-25% of BMM may be binucleate. Arrowheads highlight plasma membrane ruffles. (G) CSF1R western blot analysis showed reduced expression of the mature 165 kDa isoform in *Bcl6*−/− BMM and the presence of a potential proteolytic cleavage product with molecular mass of ~100 kDa. Lower panel, GAPDH loading control. (H) FACS analysis of surface CSF1R expression in vector-transduced *Bcl6*+/+ and *Bcl6*−/− BMM, and BCL6-reconstituted *Bcl6*−/− BMM. Bar, 10 µm.

with this, increased amounts of a possible CSF1R proteolytic cleavage product (molecular mass ~100 kDa) (Lee et al., 1999) were seen in *Bcl6*−/− BMM lysates. FACS analysis confirmed that *Bcl6*−/− BMM expressed greatly reduced levels of the CSF1R on the cell surface compared with WT macrophages and restoration of BCL6 expression significantly increased cell surface CSF1R expression in *Bcl6*−/− BMM (Fig. 8H). As BCL6 is a transcriptional repressor, upregulation of cell surface CSF1R expression by BCL6 is likely to result from an indirect effect. Despite the reported association of RasGAP with the FMS oncoprotein, we were unable to demonstrate co-immunoprecipitation of RasGAP and the CSF1R in cycling BMM in which the CSF1R is downregulated (data not shown). However, RasGAP is a well-documented binding partner of

Dok1 (Yamanashi and Baltimore, 1997), which transiently associates with the CSF1R upon CSF1 stimulation (Berg et al., 1999). Furthermore, RasGAP co-elutes with the CSF1R and Dok1 in high molecular weight, size exclusion chromatographic fractions of the phosphotyrosine-reactive fraction of CSF1-stimulated macrophages (Yeung and Stanley, 2003) (data not shown), consistent with association of RasGAP with the activated CSF1R in large protein complexes. Thus, failure of the RasGAP/RhoGAP complex to translocate to the plasma membrane in *Bcl6*−/− BMM may be due, at least in part, to reduced plasma membrane expression of the CSF1R.

CSF1R overexpression leads to reversion of the morphological phenotype in *Bcl6*−/− macrophages

As re-expression of BCL6 protein in *Bcl6*−/− BMM led to both increased expression of cell surface CSF1R and reversion of the morphological defects, we retrovirally overexpressed the CSF1R in *Bcl6*−/− BMM to delineate its role in the morphological phenotype. FACS analysis confirmed that cell surface CSF1R protein expression was elevated to levels comparable to those seen in WT BMM (Fig. 9A). The adhesion structures were examined in these cells and compared to vector-transduced *Bcl6*+/+ and *Bcl6*−/− BMM. Interestingly, increased expression of cell surface CSF1R led to reversion of the *Bcl6*−/− BMM polarization phenotype (Fig. 9B) and conversion of peripheral focal complexes to point contacts in cells expressing higher levels of GFP (Fig. 9C-I). Thus, CSF1R signaling to RhoA inactivation is downstream of BCL6 and increased surface expression of the receptor can compensate for the loss of BCL6 function in BMM adhesion and polarization.

Discussion

Previous investigations of the biological functions of BCL6 have focused on either lymphocyte differentiation and function or regulation of gene expression (Ye, 2000; Shaffer et al., 2000; Shaffer et al., 2002). The present study shows that loss of BCL6 in macrophages leads to distinctive cytoskeletal and adhesive structure abnormalities characterized by loss of polarization and defective spreading that can be largely attributed to increased Rho activation. A striking feature of *Bcl6*−/− BMM morphology was the loss of polarization (Fig. 1). Unlike the bipolar WT BMM, which usually display a broad leading lamellipodium and a trailing uropod with retraction fibers (Fig. 1C), many *Bcl6*−/− BMM either adopt a circular, spread appearance or extend multiple pseudopodia (Fig. 1B,D,F), both of which contribute to a loss of cell polarization. Further morphological examination demonstrated changes in *Bcl6*−/− BMM adhesion and actin cytoskeletal structures (Fig. 2). Y118 phospho-paxillin staining reveals that ventral surface-associated paxillin is predominantly incorporated into fine punctate structures known as point contacts rather than larger, discrete focal complexes in WT BMM. These phospho-paxillin-rich point contacts, which have been demonstrated to mediate cell spreading (Tawil et al., 1993), are often concentrated under leading lamellipodia (Fig. 2C) and may be evanescent adhesive structures similar to the transient paxillin-rich focal complexes seen at the leading edge in motile CHO cells (Laukaitis et al., 2001). In *Bcl6*−/− BMM, much of the non-

peripheral ventral surface phospho-paxillin staining is lost and these cells frequently form circumferential, radially arranged arrays of focal complexes (Fig. 2D), which may underlie circular actin structures or anchor longitudinal actin bundles (Fig. 2H). The peripheral F-actin 'belts' are condensations of the normal lamellipodial dendritic actin network (Fig. 2L).

The morphological features in the $Bcl6^{-/-}$ BMM suggested a loss of motility, the severity of which became apparent upon Boyden Chamber analysis. As the random movement or chemokinesis of these cells was significantly reduced compared with WT cells and this impairment was comparable to that seen with chemotaxis, loss of BCL6 appears to primarily affect the intrinsic motility of macrophages (Fig. 3). Lamellipodial extension and adhesion are also important in cell spreading and $Bcl6^{-/-}$ BMM were deficient in their spreading response following replating (Fig. 4). Abnormal formation of peripheral focal complexes and a severe reduction in point contact formation during spreading suggest that adhesion structure remodeling is defective in the absence of BCL6 (Fig. 4).

Instead of the widespread ventral surface point contacts seen in WT BMM, $Bcl6^{-/-}$ BMM typically display larger, peripheral focal complexes with subtended actin bundles and condensation of the cortical dendritic actin network. This is reminiscent of the Rho-stimulated conversion of focal complexes to focal adhesions in fibroblasts (Rottner et al., 1999).

Fig. 9. Overexpression of the CSF1R corrects the phenotype of $Bcl6^{-/-}$ BMM cultured in CSF1. (A) FACS analysis of surface CSF1R expression in vector-transduced $Bcl6^{+/+}$ and $Bcl6^{-/-}$ BMM, and CSF1R-transduced $Bcl6^{-/-}$ BMM. (B) Polarization indices of vector-transduced $Bcl6^{+/+}$ and $Bcl6^{-/-}$ BMM, and GFP-expressing CSF1R-transduced $Bcl6^{-/-}$ BMM (error bars, s.e.m.; *$P<0.02$ significantly different from index in $Bcl6^{+/+}$ BMM). (C-I) $Bcl6^{-/-}$ BMM overexpressing the CSF1R, as judged by high GFP levels (C, cell in the lower left corner), showed reversion of adhesion structures from peripheral focal complexes typical of $Bcl6^{-/-}$ BMM (E) to widespread ventral surface point contacts (F, cell in the lower left corner), similar to those seen in $Bcl6^{+/+}$ BMM (D). Corresponding phase-contrast images are also shown (G-I). Bar, 10 μm.

Indeed, loss of BCL6 is associated with excess RhoA activation (Fig. 5) and the $Bcl6^{-/-}$ BMM adhesion phenotype is reversible upon either re-expression of BCL6 or inhibition of Rho (Fig. 6). Consistent with our findings, increased RhoA activity has been shown previously to decrease motility in macrophages and fibroblasts (Arthur and Burridge, 2001) and polarization in fibroblasts, neutrophils and macrophages (Arthur and Burridge, 2001; Xu et al., 2003). Complete inhibition of RhoA also appears to interfere with polarization in WT and $Bcl6^{-/-}$ BMM, as has been demonstrated in fission yeast (Nakano et al., 1997). Interestingly, the C3 transferase-mediated phenotypic reversion could not be recapitulated by ROCK1 inhibition (Fig. 6). This observation is consistent with the report that mechanical force-generated maturation of focal contacts from focal complexes is Rho-dependent yet ROCK1-independent (Riveline et al., 2001). Thus, similar to the regulation of focal contact and stress fiber formation by Rho in fibroblasts, RhoA regulation of focal complex and actin bundle formation in macrophages is likely to be regulated by a ROCK1-independent RhoA effector(s) such as mDia (Riveline et al., 2001; Sahai and Marshall, 2002; Burridge and Wennerberg, 2004).

RhoGAP becomes peripherally dispersed when coexpressed with RasGAP (Trouliaris et al., 1995) and its activity towards Rho increases when complexed with RasGAP (McGlade et al., 1993; Moon and Zheng, 2003). In neutrophils, RhoGAP and RasGAP are constitutively associated and translocate to the plasma membrane during integrin-mediated spreading,
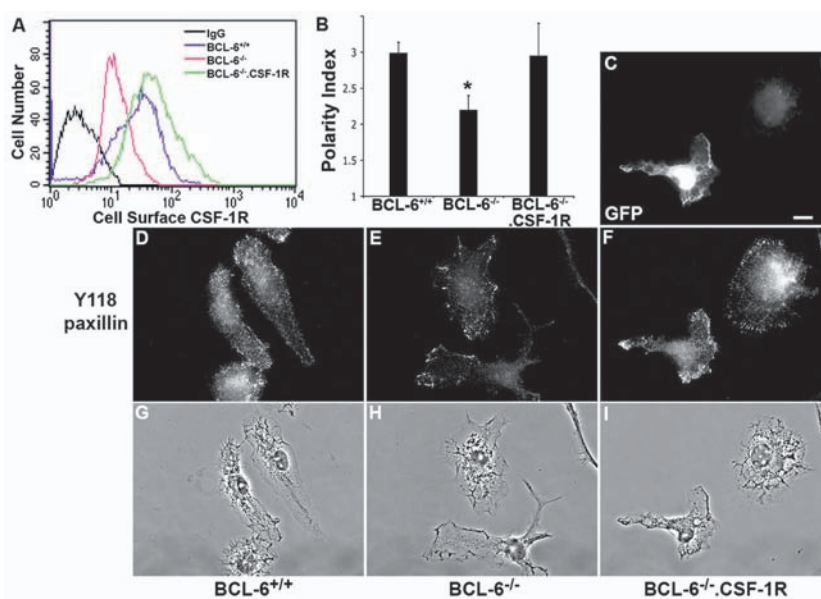
followed by a slow activation of RhoGAP and subsequent downregulation of RhoA activity (Dib et al., 2001). Consistent with the notion that RhoGAP translocation to the plasma membrane is mediated by RasGAP in macrophages, we demonstrate that decreased access of RhoGAP to RhoA at the plasma membrane is associated with reduced membrane translocation of RasGAP and reduced co-immunoprecipitation of RhoGAP by RasGAP in $Bcl6^{-/-}$ BMM (Fig. 7 and data not shown). RasGAP has been shown to associate with the activated PDGF receptor (Kazlauskas, 1994), with the oncogenic, constitutively active version of the CSF1R (*Fms*) (Trouliaris et al., 1995) and with high molecular weight, CSF1R-enriched fractions from CSF1 stimulated macrophages that also contain Dok1 (our unpublished data) (Yeung and Stanley, 2003). Thus, it is likely that translocation of the RhoGAP/RasGAP complex to the plasma membrane is mediated, at least in part, via a transient association with the activated CSF1R/Dok1 complex and, once at the membrane, RhoGAP inactivates RhoA permitting appropriate cell adhesion and efficient spreading, leading to polarization, tail retraction and normal motility. This model is supported by our findings that $Bcl6^{-/-}$ BMM express lower levels of cell surface CSF1R, have reduced plasma membrane translocation of the RhoGAP/RasGAP complex and increased RhoA activity. Consistent with a significant role for the CSF1R in the regulation of macrophage morphology and motility downstream of BCL6, re-expression of BCL6 in $Bcl6^{-/-}$ BMM increases cell surface CSF1R expression to almost WT levels

and produces complete morphological reversion, whereas overexpression of CSF1R itself in $Bcl6^{-/-}$ BMM also leads to morphological reversion. However, as elevated RhoA activity is seen in $Bcl6^{-/-}$ BMM even in the absence of CSF1 (Fig. 5B), the possibility remains that a CSF1R-independent mechanism may also contribute to this phenotype.

Overwhelming genetic evidence suggests that constitutive expression of BCL6 plays an important role in the pathogenesis of B cell lymphomas (Ye, 2000). It is also well documented that $Bcl6^{-/-}$ B cells are unable to participate in germinal center reaction (Dent et al., 1997; Fukuda et al., 1997; Ye et al., 1997). Yet, the underlying molecular mechanisms responsible for both of these processes are poorly understood. In this respect, a number of recent studies have highlighted the importance of the cytoskeleton in various lymphocyte functions, including migration, antigen recognition, signaling and activation (Vicente-Manzanares and Sanchez-Madrid, 2004). Moreover, it is clear that Rho-regulated cell adhesion and motility are directly involved in cancer cell invasion and metastasis (Sahai and Marshall, 2003). Thus, future studies are needed to address the possibility that abnormal cytoskeletal organization may contribute to a defective response of $Bcl6^{-/-}$ B cells at the onset of germinal center reaction and that B-cell lymphomas with constitutive BCL6 expression may benefit from increased cell motility during in vivo tumorigenesis.

References

Allen, W. E., Jones, G. E., Pollard, J. W. and Ridley, A. J. (1997). Rho, Rac and Cdc42 regulate actin organization and cell adhesion in macrophages. *J. Cell Sci.* **110**, 707-720.

Allen, W. E., Zicha, D., Ridley, A. J. and Jones, G. E. (1998). A role for Cdc42 in macrophage chemotaxis. *J. Cell Biol.* **141**, 1147-1157.

Arthur, W. T. and Burridge, K. (2001). RhoA inactivation by p190RhoGAP regulates cell spreading and migration by promoting membrane protrusion and polarity. *Mol. Biol. Cell* **12**, 2711-2720.

Berg, K. L., Siminovitch, K. A. and Stanley, E. R. (1999). SHP-1 regulation of p62^DOK tyrosine phosphorylation in macrophages. *J. Biol. Chem.* **274**, 35855-35865.

Boettner, B. and van Aelst, L. (2002). The role of Rho GTPases in disease development. *Gene* **286**, 155-174.

Bokoch, G. M., Bohl, B. P. and Chuang, T. H. (1994). Guanine nucleotide exchange regulates membrane translocation of Rac/Rho GTP-binding proteins. *J. Biol. Chem.* **269**, 31674-31679.

Boocock, C. A., Jones, G. E., Stanley, E. R. and Pollard, J. W. (1989). Colony-stimulating factor-1 induces rapid behavioural responses in the mouse macrophage cell line, BAC1.2F5. *J. Cell Sci.* **93**, 447-456.

Bourette, R. P. and Rohrschneider, L. R. (2000). Early events in M-CSF receptor signaling. *Growth Factors* **17**, 155-166.

Burridge, K. and Wennerberg, K. (2004). Rho and Rac take center stage. *Cell* **116**, 167-179.

Cattoretti, G., Chang, C. C., Cechova, K., Zhang, J., Ye, B. H., Falini, B., Louie, B. C., Offit, K., Chaganti, R. S. and Dalla-Favera, R. (1995). BCL6 protein is expressed in germinal-center B cells. *Blood* **86**, 45-53.

Caveggion, E., Continolo, S., Pixley, F. J., Stanley, E. R., Bowtell, D. D. L., Lowell, C. A. and Berton, G. (2003). Expression and tyrosine phosphorylation of Cbl regulates macrophage chemokinetic and chemotactic movement. *J. Cell. Physiol.* **195**, 276-289.

Cecchini, M. G., Dominguez, M. G., Mocci, S., Wetterwald, A., Felix, R., Fleisch, H., Chisholm, O., Hofstetter, W., Pollard, J. W. and Stanley, E. R. (1994). Role of colony stimulating factor-1 in the establishment and regulation of tissue macrophages during postnatal development of the mouse. *Development* **120**, 1357-1372.

Coleman, M. L., Sahai, E. A., Yeo, M., Bosch, M., Dewar, A. and Olson, M. F. (2001). Membrane blebbing during apoptosis results from caspase-mediated activation of ROCK I. *Nat. Cell Biol.* **3**, 339-345.

Dent, A. L., Shaffer, A. L., Yu, X., Allman, D. and Staudt, L. M. (1997). Control of inflammation, cytokine expression, and germinal center formation by BCL6. *Science* **276**, 589-592.

Dib, K., Melander, F. and Andersson, T. (2001). Role of p190RhoGAP in β_2 integrin regulation of RhoA in human neutrophils. *J. Immunol.* **166**, 6311-6322.

Ellis, C., Moran, M., McCormick, F. and Pawson, T. (1990). Phosphorylation of GAP and GAP-associated proteins by transforming and mitogenic tyrosine kinases. *Nature* **343**, 377-381.

Etienne-Manneville, S. and Hall, A. (2002). Rho GTPases in cell biology. *Nature* **420**, 629-635.

Fukuda, T., Yoshida, T., Okada, S., Hatano, M., Miki, T., Ishibashi, K., Okabe, S. Koseki, H., Hirosawa, S., Taniguchi, M. et al. (1997). Disruption of the Bcl6 gene results in an impaired germinal center formation. *J. Exp. Med.* **186**, 439-448.

Gardiner, E. M., Pestonjamasp, K. N., Bohl, B. P., Chamberlain, C., Hahn, K. and Bokoch, G. M. (2002). Spatial and temporal analysis of Rac activation during live neutrophil chemotaxis. *Curr. Biol.* **12**, 2029-2034.

Hartwig, J. H. (1992). Mechanisms of actin rearrangements mediating platelet activation. *J. Cell Biol.* **118**, 1421-1442.

Kazlauskas, A. (1994). Receptor tyrosine kinases and their targets. *Curr. Opin. Genet. Dev.* **4**, 5-14.

Kusam, S., Toney, L. M., Sato, H. and Dent, A. L. (2003). Inhibition of Th2 differentiation and GATA-3 expression by BCL6. *J. Immunol.* **170**, 2435-2441.

Laukaitis, C. M., Webb, D. J., Donais, K. and Horwitz, A. F. (2001). Differential dynamics of alpha 5 integrin, paxillin, and alpha-actinin during formation and disassembly of adhesions in migrating cells. *J. Cell Biol.* **153**, 1427-1440.

Lee, P. S. W., Wang, Y., Dominguez, M. G., Yeung, Y.-G., Murphy, M. A., Bowtell, D. D. L. and Stanley, E. R. (1999). The Cbl protooncoprotein stimulates CSF-1 receptor multiubiquitination and endocytosis, and attenuates macrophage proliferation. *EMBO J.* **18**, 3616-3628.

McGlade, J., Brunkhorst, B., Anderson, D., Mbamalu, G., Settleman, J., Dedhar, S., Rozakis-Adcock, M., Chen, L. B. and Pawson, T. (1993). The N-terminal region of GAP regulates cytoskeletal structure and cell adhesion. *EMBO J.* **12**, 3073-3081.

Meili, R. and Firtel, R. A. (2003). Two poles and a compass. *Cell* **114**, 153-156.

Moon, S. Y. and Zheng, Y. (2003). Rho GTPase-activating proteins in cell regulation. *Trends Cell Biol.* **13**, 13-22.

Muller, A. J., Young, J. C., Pendergast, A.-M., Pondel, M., Landau, N. R., Littman, D. R. and Witte, O. N. (1991). BCR first exon sequences specifically activate the BCR/ABL tyrosine kinase oncogene of Philadelphia Chromosome-positive human leukemias. *Mol. Cell. Biol.* **11**, 1785-1792.

Nakano, K., Arai, R. and Mabuchi, I. (1997). The small GTP-binding protein Rho1 is a multifunctional protein that regulates actin localization, cell polarity, and septum formation in the fission yeast Schizosaccharomyces pombe. *Genes Cells.* **2**, 679-694.

Neumeister, P., Pixley, F. J., Xiong, Y., Xie, H., Wu, K., Ashton, A., Cammer, M., Chan, A., Symons, M., Stanley, E. R. et al. (2003). Cyclin D1 governs adhesion and motility of macrophages. *Mol. Biol. Cell* **14**, 2005-2015.

Persons, D. A., Allay, J. A., Allay, E. R., Ashmun, R. A., Orlic, D., Jane, S. M., Cunningham, J. M. and Nienhuis, A. W. (1999). Enforced

expression of the GATA-2 transcription factor blocks normal hematopoiesis. *Blood* **93**, 488-499.

Pixley, F. J., Lee, P. S. W., Condeelis, J. S. and Stanley, E. R. (2001). Protein tyrosine phosphatase φ regulates paxillin tyrosine phosphorylation and mediates colony-stimulating factor 1-induced morphological changes in macrophages. *Mol. Cell. Biol.* **21**, 1795-1809.

Pixley, F. J. and Stanley, E. R. (2004). CSF-1 regulation of the wandering macrophage: complexity in action. *Trends Cell Biol.* **14**, 628-638.

Ren, X. D., Kiosses, W. B. and Shwartz, M. A. (1999). Regulation of the small GTP-binding protein Rho by cell adhesion and the cytoskeleton. *EMBO J.* **18**, 578-585.

Ridley, A. (2001). Rho GTPases and cell migration. *J. Cell Sci.* **114**, 2713-2722.

Ridley, A., Schwartz, M. A., Burridge, K., Firtel, R. A., Ginsberg, M. H., Borisy, G., Parsons, J. T. and Horwitz, A. R. (2003). Cell migration: integrating signals from front to back. *Science* **302**, 1704-1709.

Riveline, D., Zamir, E., Balaban, N. Q., Schwartz, U. S., Ishizaki, T., Narumiya, S., Kam, Z., Geiger, B. and Bershadsky, A. D. (2001). Focal contacts as mechanosensors: externally applied local mechanical force induces growth of focal contacts by an mDia-dependent and ROCK-independent mechanism. *J. Cell Biol.* **153**, 1175-1185.

Rottner, K., Hall, A. and Small, J. V. (1999). Interplay between rac and rho in the control of substrate contact dynamics. *Curr. Biol.* **9**, 640-648.

Sahai, E. and Marshall, C. J. (2002). Rho-GTPases and cancer. *Nat. Rev. Cancer* **2**, 133-142.

Sahai, E. and Marshall, C. J. (2003). Differing modes of tumour cell invasion have distinct requirements for Rho/ROCK signalling and extracellular proteolysis. *Nat. Cell Biol.* **5**, 711-719.

Shaffer, A. L., Yu, X., He, Y., Boldrick, J., Chan, E. P. and Staudt, L. M. (2000). BCL-6 represses genes that function in lymphocyte differentiation, inflammation, and cell cycle control. *Immunity* **13**, 199-212.

Shaffer, A. L., Rosenwald, A. and Staudt, L. M. (2002). Lymphoid malignancies: the dark side of B-cell differentiation. *Nat. Rev. Immunol.* **2**, 920-932.

Shaw, R. J., Henry, M., Solomon, F. and Jacks, T. (1998). RhoA-dependent phosphorylation and relocalization of ERM proteins into apical membrane/actin protrusions in fibroblasts. *Mol. Biol. Cell* **9**, 403-419.

Stanley, E. R. (1990). Murine bone marrow-derived macrophages. *Methods Mol. Biol.* **75**, 301-304.

Stanley, E. R., Berg, K. L., Einstein, D. B., Lee, P. S. W., Pixley, F. J., Wang, Y. and Yeung, Y. G. (1997). Biology and action of colony-stimulating factor-1. *Mol. Reprod. Dev.* **46**, 4-10.

Sudo, T., Nishikawa, S., Ogawa, M., Kataoka, H., Ohno, N., Izawa, A., Hayashi, S. and Nishikawa, S. (1995). Functional hierarchy of c-kit and c-fms in intramarrow production of CFU-M. *Oncogene* **11**, 2469-2476.

Suen, P. W., Ilic, D., Caveggion, E., Berton, G., Damsky, C. H. and Lowell, C. A. (1999). Impaired integrin-mediated signal transduction, altered cytoskeletal structure and reduced motility in Hck/Fgr deficient macrophages. *J. Cell Sci.* **112**, 4067-4078.

Svitkina, T. M., Verkhovsky, A. B. and Borisy, G. G. (1995). Improved procedures for electron microscopic visualization of the cytoskeleton of cultured cells. *J. Struct. Biol.* **115**, 290-303.

Tawil, N., Wilson, P. and Carbonetto, S. (1993). Integrins in point contacts mediate cell spreading: factors that regulate integrin accumulation in point contacts vs. focal contacts. *J. Cell Biol.* **120**, 261-271.

Toney, L. M., Cattoretti, G., Graf, J. A., Merghoub, T., Pandolfi, P. P., Dalla-Favera, R., Ye, B. H. and Dent, A. L. (2000). BCL6 regulates chemokines gene transcription in macrophages. *Nat. Immunol.* **1**, 214-220.

Trouliaris, S., Smola, U., Chang, J.-H., Parsons, S. J., Niemann, H. and Tamura, T. (1995). Tyrosine 807 of the v-fms oncogene product controls cell morphology and association with p120RasGAP. *J. Virol.* **69**, 6010-6020.

Tushinski, R. J., Oliver, I. T., Guilbert, L. J., Tynan, P. W., Warner, J. R. and Stanley, E. R. (1982). Survival of mononuclear phagocytes depends on a lineage-specific growth factor that the differentiated cells selectively destroy. *Cell* **28**, 71-81.

Vicente-Manzanares, M. and Sanchez-Madrid, F. (2004). Role of the cytoskeleton during leukocyte responses. *Nat. Rev. Immunol.* **4**, 110-122.

Wang, Y., Yeung, Y. G. and Stanley, E. R. (1999). CSF-1 stimulated multiubiquitination of the CSF-1 receptor and of Cbl follows their tyrosine phosphorylation and association with other signaling proteins. *J. Cell. Biochem.* **72**, 119-134.

Webb, S. E., Pollard, J. W. and Jones, G. E. (1996). Direct observation and quantification of macrophage chemoattraction to the growth factor CSF-1. *J. Cell Sci.* **109**, 793-803.

Worthylake, R. A., Lemoine, S., Watson, J. M. and Burridge, K. (2001). RhoA is required for monocyte tail retraction during transendothelial migration. *J. Cell Biol.* **154**, 147-160.

Xu, J., Wang, F., van Keymeulen, A., Herzmark, P., Straight, A., Kelly, K., Takuwa, Y., Sugimoto, N., Mitchison, T. and Bourne, H. R. (2003). Divergent signals and cytoskeletal assemblies regulate self-organizing polarity in neutrophils. *Cell* **114**, 201-214.

Yamanashi, Y. and Baltimore, D. (1997). Identification of the Abl- and rasGAP-associated 62 kD protein as a docking protein, Dok. *Cell* **88**, 205-211.

Yamochi, T., Kitabayashi, A., Hirokawa, M., Miura, A. B., Onizuka, T., Mori, S. and Moriyama, M. (1997). Regulation of the BCL6 gene expression in human myeloid/monocytoid leukemic cells. *Leukemia* **11**, 694-700.

Ye, B. H. (2000). BCL6 in the pathogenesis of non-Hodgkin's lymphoma. *Cancer Invest.* **18**, 356-365.

Ye, B. H., Cattoretti, G., Shen, Q., Zhang, J., Hawe, N., de Waard, R., Leung, C., Nouri-Shirazi, M., Orazi, A., Chaganti, R. S. et al. (1997). The BCL-6 proto-oncogene controls germinal-centre formation and Th2-type inflammation. *Nat. Genet.* **16**, 161-170.

Yeung, Y.-G. and Stanley, E. R. (2003). Proteomic approaches to the analysis of early events in CSF-1 signal transduction. *Mol. Cell. Proteomics* **2**, 1143-1155.